This article was downloaded by:
On: *21 January 2011*
Access details: *Access Details: Free Access*
Publisher *Taylor & Francis*
Informa Ltd Registered in England and Wales Registered Number: 1072954 Registered office: Mortimer House, 37-41 Mortimer Street, London W1T 3JH, UK

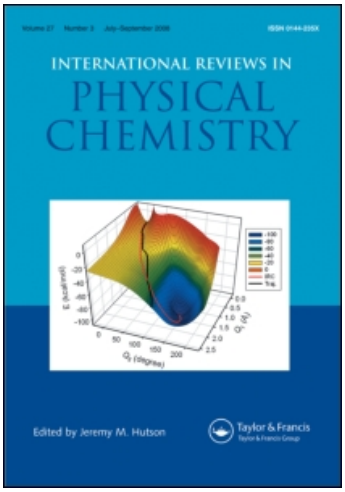

International Reviews in Physical Chemistry
Publication details, including instructions for authors and subscription information:
http://www.informaworld.com/smpp/title~content=t713724383

Sum frequency generation spectroscopy of the aqueous interface: Ionic and soluble molecular solutions

Mary Jane Shultz; Cheryl Schnitzer; Danielle Simonelli; Steve Baldelli

Online publication date: 26 November 2010

To cite this Article Shultz, Mary Jane , Schnitzer, Cheryl , Simonelli, Danielle and Baldelli, Steve(2000) 'Sum frequency generation spectroscopy of the aqueous interface: Ionic and soluble molecular solutions', International Reviews in Physical Chemistry, 19: 1, 123 — 153
To link to this Article: DOI: 10.1080/014423500229882
URL: http://dx.doi.org/10.1080/014423500229882

PLEASE SCROLL DOWN FOR ARTICLE

Full terms and conditions of use: http://www.informaworld.com/terms-and-conditions-of-access.pdf

This article may be used for research, teaching and private study purposes. Any substantial or systematic reproduction, re-distribution, re-selling, loan or sub-licensing, systematic supply or distribution in any form to anyone is expressly forbidden.

The publisher does not give any warranty express or implied or make any representation that the contents will be complete or accurate or up to date. The accuracy of any instructions, formulae and drug doses should be independently verified with primary sources. The publisher shall not be liable for any loss, actions, claims, proceedings, demand or costs or damages whatsoever or howsoever caused arising directly or indirectly in connection with or arising out of the use of this material.

INT. REVIEWS IN PHYSICAL CHEMISTRY, 2000, VOL. 19, NO. 1, 123–153

Sum frequency generation spectroscopy of the aqueous interface: ionic and soluble molecular solutions

MARY JANE SHULTZ, CHERYL SCHNITZER, DANIELLE SIMONELLI
Department of Chemistry, Pearson Laboratory, Tufts University, Medford, MA 02155, USA

and STEVE BALDELLI
Department of Chemistry, University of California, Berkeley, CA 94720, USA

Downloaded At: 16:53 21 January 2011

The liquid interface of aqueous solutions is of central importance to numerous phenomena from cloud processing of combustion generated oxides to corrosion degradation of structural materials to transport across cell membranes. Despite the importance of this interface, little molecular-level information was known about it prior to the last decade-and-a-half. Molecular-level information is important not only for a fundamental understanding of processes at interfaces, but also for predicting methods for diminishing deleterious effects. Recently, the nonlinear spectroscopic method, sum frequency generation (SFG), has been applied to the investigation of the structure of the liquid interface. This review focuses on the liquid–air interface of aqueous solutions containing soluble, ionic species—H_2SO_4, HNO_3, HCl, alkali sulphates and bisulphates, NaCl and $NaNO_3$—as well as soluble molecular species—glycerol, sulphuric acid and ammonia. Ionic materials influence the structure of water at the interface through an electric double layer which arises from the differential distribution of anions and cations near the interface. Due to the extreme size of the proton, the strongest field is generated by acidic materials. As the concentration of these ionic materials increases, ion pairs form diminishing the strength of the double layer. This enables the ion-pair complex to penetrate to the interface and either displace water or bind it into hydrated complexes. Soluble materials of lower surface tension partition to the interface and either displace water from the interface or bind water into hydrated complexes. In particular, the conjectured ammonia–water complex on aqueous solutions is observed and it is determined to tilt 34–38° from the normal.

Contents

International Reviews in Physical Chemistry ISSN 0144-235X print/ ISSN 1366-591X online
© 2000 Taylor & Francis Ltd http://www.tandf.co.uk/journals/tf/0144235X.html

Downloaded At: 16:53 21 January 2011

1. Background

1.1. *The liquid interface*

Liquid interfaces are ubiquitous in nature. For example, the surface of cloud droplets are clearly liquid interfaces. However, there is evidence that even ice crystals or 'dry' sea salt aerosols are covered with a layer of liquid or liquid-like water. In addition, nearly all metal surfaces exposed to ambient air are coated with at least a layer of water which assists the corrosion process. Biological systems contain numerous liquid–solid and liquid–air interfaces, including cell walls and the surfaces of large proteins, DNA, etc. Thus, unravelling the basis for issues as diverse as the chemistry of ozone depletion, corrosion, macromolecular protein conformation, or transport across cell membranes requires a fundamental, molecular-level understanding of liquid interfaces.

Despite the importance of the liquid interface in general, and that of water specifically, experimental molecular-level data was almost totally lacking prior to the last decade and a half. Measurements such as surface tension and surface potential provide a macroscopic model of the interface including concepts such as the excess of one component in a binary mixture at the interface. However, answering deceptively simple questions such as, 'What is the structure of water at the neat water interface?' or 'In a ternary mixture, which components form the surface monolayer?' cannot be answered with these techniques.

Methods used successfully in forming detailed pictures of solid surfaces cannot answer similar questions about many liquid interfaces since most solid state techniques require an ultrahigh vacuum to diminish gas-phase scattering. Indeed, the liquid interfaces that have been probed with scattering techniques [1, 2, 3] are low vapour pressure interfaces. Linear spectroscopic techniques such as total internal reflection infrared or electronic spectroscopy suffer from poor spatial resolution since the evanescent wave penetrates about 1000 Å, too far for interface-specific data unless the probed molecule is restricted to the surface. But of course, that is part of the question which needs to be answered in most cases.

This situation began to change about a decade-and-a-half ago due to development of two nonlinear spectroscopic techniques—second harmonic generation (SHG) and sum frequency generation (SFG). Both are three-wave mixing processes that originate from the rapid change of index of refraction which occurs at an interface. If the two input waves are sufficiently intense, their interference generates a nonlinear polarization at the sum and difference frequencies. With the two input waves at the same frequency (ω), the generated polarization oscillates at the harmonic frequency (2ω)—this is second harmonic generation. If the two are not the same (ω_1 and ω_2) then the outputs are at the sum ($\omega_1 + \omega_2$) and difference ($\omega_1 - \omega_2$) frequencies. Applications discussed in this paper utilize the sum frequency. Further, if one of the inputs is an infrared frequency, then the sum frequency is resonance enhanced when a vibrational mode of the interfacial molecules matches the frequency of the input. Detection of the vibrational resonances is facilitated since the sum frequency is in the visible region.

This paper focuses specifically on SFG results on water and aqueous interfaces. It is organized as follows. The balance of this section outlines development of the technique and early results for substances expected to partition to the interface on aqueous solutions. In the second half, more recent results with molecules which are miscible with water are examined. The theoretical basis of SFG is subsequently described, including the polarization analysis for determining oscillator orientation. The polarization analysis is applied to specific molecules in sections 3 and 4, which concentrates on results from our laboratory. These include the effect of small inorganic ions on the structure of interfacial water molecules [4–9] as well as partitioning and orientation of small soluble molecules at the interface [5, 6, 8, 10–14]. It includes a discussion of the electric double layer model applied to understand the effect of ions in solution on the structure of surface water. The last section is a summary.

Downloaded At: 16:53 21 January 2011

1.2. *Technique development*

As indicated above, probing liquid interfaces is challenging due to the inherently dynamic nature of the surface. For example, at 0°C the vapour pressure of water (~4.5 Torr) results in an exchange of about a monolayer every 300 ns between the gas phase and the surface. In this sense, it is a bit surprising that a spectrum of the surface contains features other than very broad bands due to the ever changing environment. The resonances therefore reflect the orientational effect of the asymmetric environment at the surface.

The basis for the two nonlinear techniques was set out by Bloembergen and Pershan in the 1960s [15] and several reviews have since appeared in the literature [16–19]. The following is an outline of the development of these techniques. It was not until the late 1980s that the nonlinear spectroscopy described by Bloembergen was applied to liquid interfaces. The first SHG experiments were reported by Shen and co-workers and involved *p*-nitrobenzoic acid [20]. The combination of the polarizability of the nitro group and that of the phenyl π-system results in a large SHG cross-section making this an excellent proof-of-concept system. Since SHG involves only one frequency input, it is experimentally simpler to implement than SFG. The experimental simplicity comes at the cost of difficulty in interpretation since the molecular polarizability is the result of summation over many electronic states. Interpretation of the results is greatly facilitated by accessing molecular

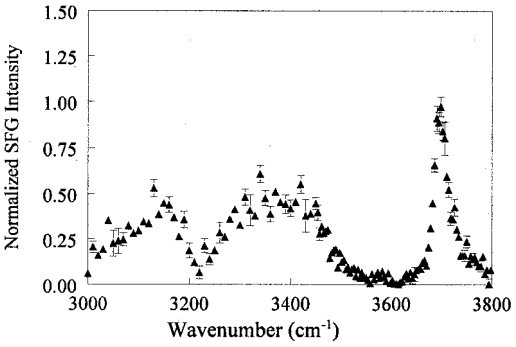

Figure 1. Sum frequency spectrum of water with s-polarized sum frequency, s-polarized visible, and p-polarized infrared beams.

resonances so that few molecular states contribute significantly to the polarizability. This is the basis for tuning the input so that the fundamental or second harmonic is in resonance with an electronic state [21]. This strategy, however, diminishes general applicability of the technique since not all molecules have suitable electronic resonances well separated from other molecules in a mixture.

To retain general applicability and access resonances, two input frequencies can be used—one in the infrared and one in the visible. Vibrational resonances facilitate interpretation of results, now at the cost of experimental complexity. As discussed below, the major complexity arises in generating tunable infrared frequencies of sufficient intensity to drive the nonlinear polarization. (Difficulties in generating high-power, tunable infrared is one reason for the lack of second harmonic experiments relying on infrared excitation.) The first SFG experiments, reported in 1987–1988, involved organic molecules on solid substrates: quartz [22, 23] and semiconductors [24].

The first reported results on a neat liquid interface is the SHG of water by Eisenthal and co-workers [25]. Analysis of the polarization dependence of the output indicates that the average dipole moment vector of interfacial water is nearly parallel to the interface and points slightly toward the bulk, i.e. on average, the hydrogen atoms are oriented slightly below the surface. SFG spectra of neat liquid interfaces followed several years later, beginning with methanol by Shen and co-workers [26], followed by that of pure water in 1993 [27]. Thus, SFG investigations of aqueous interfaces have been ongoing for less than a decade. SFG is the only current technique that can yield a vibrational spectrum of a neat liquid interface. The vibrational nature of the spectrum is significant since it furnishes details that are not possible with any other spectroscopy. As an example, consider the spectrum of pure water, shown in figure 1, taken in our laboratory. Although of higher resolution, it is in good agreement with that of Shen and co-workers. The resonances provide detailed information about interfacial water. For example, the peak at 3700 cm^{-1} is due to an O–H oscillator free of hydrogen bonding. (Hereafter referred to as a 'free OH'.) This frequency is at the uncoupled OH oscillator frequency, i.e. midway between the symmetric and antisymmetric gas-phase peaks of water. Since the frequency is unperturbed from the free-OH oscillator and is relatively narrow, it must originate from water molecules in the first layer with the hydrogen atom directed toward the gas phase. This proves that SFG can sense the top monolayer of the surface in the

Downloaded At: 16:53 21 January 2011

presence of much larger numbers of molecules in the adjacent bulk phases. It is estimated that the free OH accounts for ~20% of a monolayer [27]. The remaining resonances provide information on hydrogen-bonded water molecules and will be discussed further below.

1.3. *Molecular orientation on aqueous surfaces*

1.3.1. *Water immiscible molecules*

Determining the orientation of solute molecules at the aqueous interface is important for understanding reactions at the liquid surface, particularly catalytic processes or transport across an interface. Most reports of orientation have used SHG, exploiting the polarization dependence of the output. A few, however, have coupled the vibrational and polarization information provided by SFG to determine orientation of specific oscillators at the surface. The first of these investigated acid ionization of alkyl phenols and anilines at the surface [28]. The results show that the interfacial pH differs from that in the bulk. This is perhaps not surprising since energetics favour the neutral form at the interface. More significantly, the difference between the bulk and surface pK_a depends on the chain length linking the localized charge with the aromatic, hydrophobic moiety. The bulk and surface pK_a are nearly the same if the ionic end is ~5 layers into the bulk [29, 30]. This result has significant implications for the energetics of ions near the interface—a topic of discussion in section 3.3.

Downloaded At: 16:53 21 January 2011

On aqueous surfaces, many molecules are tilted at approximately 40° where the tilt angle is measured relative to the surface normal. The first orientation results were reported for *p*-nitrobenzoic acid which is tilted by 40° on water [20]. Similarly, *p*-nitrophenol is tilted 40° from the normal [31]. A larger tilt angle, 50°, was found for phenol which maintains this orientation up to one monolayer after which it lies flatter [32]. These results are for water in contact with air. Replacing air with a non-polar molecule, CCl_4, does not alter the propensity to 40°. Sodium 1-dodecylnaphthalene-4-sulphonat e at the water–CCl_4 interface is found to tilt 34–38° off the normal [33].

All of the results indicated in the previous paragraph, were obtained by examining the polarization characteristics of the SHG signal. The power of access to vibrational information is illustrated by a recent report [34] of the orientation of 4″-*n*-pentyl-4-cyano-*p*-terphenyl ($CH_3(CH_2)_4(C_6H_4)_3CN$) (PCT). Long-chain molecules have the potential for different orientations for the portion in contact with water and that extending into the gas phase. PCT can be subdivided into three parts: the cyanide moiety, the terphenyl ring system, and the alkyl chain. The vibrational information provided by SFG is necessary to determine the orientation of the cyanide and the terminal methyl groups in the presence of the much larger polarizability of the terphenyl system. With the cyanide and methyl groups fixed, the SHG response is used to determine the orientation of the terphenyl system. The combination, provides detailed information about orientation on the aqueous interface. The deduced orientation depends on the index of refraction of the local medium, n'. Arbitrarily assuming $n' = 1.18$ indicates that the cyanide moiety is tilted 50° off the normal. Assuming an index closer to that of water, a reasonable assumption given that the cyanide group is likely to be imbedded in water, results in a smaller angle. The terphenyl system is tilted just over 50° and the C_3 axis of the methyl group is tilted 39°. Although some details remain, this work demonstrates the considerable power of these nonlinear techniques.

A common characteristic of the early systems investigated by SHG as well as that of PCT discussed above, is that they involve molecules which are sufficiently hydrophobic that they are expected to preferentially partition to the surface of water. The forces that determine the molecular orientation are therefore a combination of the hydrogen-bonding interaction at one end of the molecule and the hydrophobic interaction due to the remainder of the molecule.

1.3.2. *Water miscible molecules*

Molecules that are miscible with water present the potential for a very different orientation on the aqueous surface since the interaction must necessarily be stronger for the two to be miscible. The first analysis of the orientation of a molecule miscible with water is that of acetonitrile [35]. For bulk mole fraction, x, up to 0.07, the cyanide axis is tilted 40° from the normal. The tilt angle increases to 70° for larger bulk mole fractions. This suggests that acetonitrile, although miscible, significantly partitions to the interface and forms a monolayer at $x = 0.07$. Hence, up to a monolayer, interaction with surface water molecules again dictates the orientation as tilted 40°.

Recently, we have determined the orientation of a very soluble molecule, ammonia. This work, discussed further below, is the first report of the orientation of a gas-phase molecule on an aqueous surface. Similar to many molecules, ammonia is tilted 34–38° off the normal [10, 12, 13]. The orientation of ammonia on solid surfaces has been determined by numerous other techniques and it is often oriented with the C_3 axis perpendicular to the surface. So the non-normal orientation of ammonia is unusual.

These orientation results suggest that the hydrogen-bonding network of water is rather robust dictating the orientation of a wide variety of molecules which preferentially link to the aqueous surface through one site. More systems need to be investigated before further conclusions can be drawn about the integrity of this hydrogen-bonded network.

Downloaded At: 16:53 21 January 2011

2. Technique description

2.1. *Theoretical underpinnings*

The following is a presentation of the basis for SFG. Readers interested in greater detail are referred to the classic paper by Bloembergen and Pershan [15] or subsequent treatments [36–41]. The nonlinear response of the medium to the input waves is determined by the hyperpolarizability of the medium. The incident waves induce a polarization, **P**,

$$\mathbf{P} = \alpha^{(1)} \cdot \mathbf{E} + \chi^{(2)} : \mathbf{E}_1\mathbf{E}_2 + \cdots, \tag{1}$$

where $\alpha^{(1)}$ and $\chi^{(2)}$ are the first and second order polarizability respectively. The direction of the incident electric field, **E**, and the polarization are not necessarily the same. Thus, the first order response, $\alpha^{(1)}$, is a matrix. It describes Raleigh and Raman scattering. The second order response is a tensor which is the focus of this discussion. Equation (1) implies that there are two relationships which must be considered to understand this second order response: the relationship of the electric fields, $\mathbf{E}_1$, $\mathbf{E}_2$ in the nonlinear medium to the incident fields, and the relationship of the second order polarizability tensor, $\chi^{(2)}$, to the molecules in the surface. Each of these is described below.

2.1.1. *Optical factors and electric fields*

The electric fields in the medium are related to the incident fields by Fresnel factors which reflect the efficiency for coupling into the nonlinear medium. There is a similar optical factor for coupling the generated sum frequency out. These factors are a direct result of the boundary condition on a light wave at the interface between two different media—the tangential component of the electric field is continuous across the boundary. As a result of this boundary condition, the coupling efficiency for light polarized in the plane of incidence, p-polarized, is larger than that polarized perpendicular to the plane, s-polarized. Furthermore, for p-polarized light, the efficiency of each of the two components (parallel and perpendicular to the surface) depends on the angle of incidence, plus the normal component has a phase shift. This polarization dependence complicates the analysis, however, it also is the basis for determining orientational information.

In many cases, the liquid interface is isotropic in the surface plane. Surface isotropy reduces the eight potential polarization combinations to four that are non-zero: ssp, sps, pss, and ppp. Note: the now common convention for the order of the indices is sum frequency, visible, infrared. The four, non-zero sum frequency intensities are:

$$I_{\mathrm{ssp}} \propto \left|a_{YYZ}\chi_{YYZ}\right|^2; \quad I_{\mathrm{sps}} \propto \left|a_{YZY}\chi_{YZY}\right|^2; \quad I_{\mathrm{pss}} \propto \left|a_{ZYY}\chi_{ZYY}\right|^2, \tag{2}$$

$$I_{\mathrm{ppp}} \propto \left|a_{XXZ}\chi_{XXZ} + a_{XZX}\chi_{XZX} + a_{ZXX}\chi_{ZXX} + a_{ZZZ}\chi_{ZZZ}\right|^2, \tag{3}$$

where χ_{IJK} are the nonlinear susceptibilities discussed further below and

$$a_{IJK} = e_I(\mathrm{SF})e_J(\mathrm{vis})e_K(\mathrm{IR}). \tag{4}$$

The e_I fields in equation (4) are related to the input fields by

$$e_I(\mathrm{SF}) = L_I(\mathrm{SF}); \quad e_J(\mathrm{vis}) = K_J(\mathrm{vis})e^{\circ}(\mathrm{vis}); \quad e_K(\mathrm{IR}) = K_J(\mathrm{IR})e^{\circ}(\mathrm{IR}), \tag{5}$$

where the optical and Fresnel factors: $L_I(\mathrm{SF})$, $K_J(\mathrm{vis})$, $K_K(\mathrm{IR})$ for the sum frequency, visible, and infrared wavelengths respectively are listed in table 1 and $e^{\circ}(\mathrm{vis})$ ($e^{\circ}(\mathrm{IR})$) is the incident visible (infrared) field. In the table θ_{i} (θ_{t}) is the incident (transmitted) angle. The transmitted angle is related to the incident angle by Snell's Law.

Utilization of the Fresnel factors requires calculation of the sum frequency angle. This is determined by momentum matching at the interface.

$$n_{\mathrm{SF}}^2\omega_{\mathrm{SF}}^2 \sin^2\theta_{\mathrm{SF}} = n_1^2\omega_1^2 \sin^2\theta_1 + n_2^2\omega_2^2 \sin^2\theta_2 + n_1 n_2 \omega_1 \omega_2 \sin\theta_1 \sin\theta_2. \tag{6}$$

The Fresnel factors reduce the electric fields. In addition, for the ppp polarization combination, interference between the components indicated in equation (3) can result in alteration or cancellation of expected intensities.

2.1.2. *Nonlinear susceptibility*

The relationship between the surface nonlinear susceptibility, χ_{IJK}, and the molecular hyperpolarizability, β_{abc}, is the key to utilizing polarization data from SFG experiments to determine molecular orientation. Briefly, it involves projecting the molecular hyperpolarizability onto the laboratory coordinate system for each molecule in the surface and determining the resultant polarization. In detail, this is an exercise in Euler angle relationships among four coordinate systems: the laboratory system which defines the plane of incidence, the surface system which defines the surface normal (for aqueous systems, the surface is isotropic), the molecular

Downloaded At: 16:53 21 January 2011

Table 1. Fresnel factors. X, Y, and Z are the laboratory coordinate system where XZ is the plane of incidence and XY is the surface plane.

	L(SF)
X	$-\cos\theta_{t,SF}/[\cos\theta_{t,SF} + n_{SF}\cos\theta_{i,SF}]$
Y	$1/[\cos\theta_{i,SF} + n_{SF}\cos\theta_{t,SF}]$
Z	$-\sin\theta_t/[\cos\theta_{t,SF} + n_{SF}\cos\theta_{i,SF}]$
	K(vis)
X	$2\cos\theta_{i,\omega1}\cos\theta_{t,\omega1}/[\cos\theta_{t,\omega1} + n_1\cos\theta_{i,\omega1}]$
Y	$2\cos\theta_{i,\omega1}/[\cos\theta_{i,\omega1} + n_1\cos\theta_{t,\omega1}]$
Z	$-2\cos\theta_{i,\omega1}\sin\theta_{t,\omega1}/[\cos\theta_{t,\omega1} + n_1\cos\theta_{i,\omega1}]$
	K(IR)
X	$2\cos\theta_{i,\omega2}\cos\theta_{t,\omega2}/[\cos\theta_{t,\omega2} + n_2\cos\theta_{i,\omega2}]$
Y	$2\cos\theta_{i,\omega2}/[\cos\theta_{i,\omega2} + n_2\cos\theta_{t,\omega2}]$
Z	$-2\cos\theta_{i\omega2}\sin\theta_{t\omega2}/[\cos\theta_{t,\omega2} + n_2\cos\theta_{i,\omega2}]$

Table 2. Notation for coordinate systems and hyperpolarizability.

	Laboratory	Surface	Molecular Cartesian	Molecular normal mode
Coordinates	XYZ	xyz	abc	ABC
Hyperpolarizability	χ_{IJK}	χ_{ijk}	β_{abc}	β_{ABC}

Downloaded At: 16:53 21 January 2011

Cartesian system, and the molecular normal coordinates. The general results of these transformations are given in the literature [38, 39]. Only a brief discussion of aspects pertaining to isotropic liquid interfaces is given here. As an aid in tracing the projection, the notation for the four coordinate system is listed in table 2. The same notation is used throughout this paper.

The following is an outline of the transformation beginning with the molecular normal mode coordinate system, ABC. Transformation from normal mode coordinates to molecular Cartesian coordinates is non-trivial only for degenerate vibrational modes. For degenerate modes, there are multiple, equivalent molecular orientations with respect to the Cartesian coordinate system. The Cartesian susceptibility elements are related to the normal coordinate elements as

$$\beta_{abc} = \frac{1}{n}\sum_{\text{orientations}}\beta_{ABC}, \tag{7}$$

where n is the number of equivalent orientations. Each of these Cartesian coordinate susceptibilities are projected onto the surface coordinate system and averaged over the equivalent surface orientations.

$$\chi_{IJK} = N\langle\beta_{IJK}\rangle, \tag{8}$$

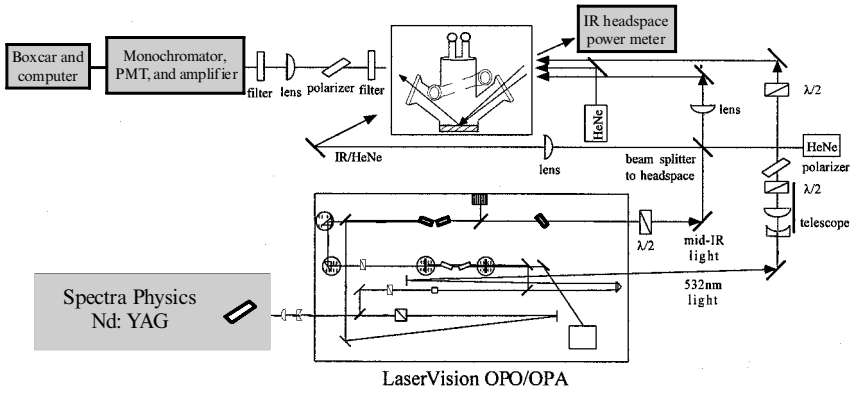

Figure 2. Experimental set-up.

where N is the number of molecules and $\langle \cdots \rangle$ denotes the orientational average. For an isotropic surface, all rotation angles within the surface plane are equally likely. It is this random, surface-plane orientation which results in zero intensity for sss, spp, psp and pps polarization. In general, there remain two angles which specify the projection of the molecular Cartesian axes onto the surface: a tilt and a twist angle, θ and ϕ, respectively. For one-dimensional modes, e.g. the free OH of water, all twists are equivalent. Thus, the SF intensity depends only on the tilt angle. The twenty seven elements of the hyperpolarizability tensor reduce to four non-zero elements:

$$\chi_{XXZ} = \cos\theta\,\beta_{aac} + \tfrac{1}{2}(\cos\theta - \cos^3\theta)(\beta_{ccc} - \beta_{aac}), \tag{9}$$

$$\chi_{xzx} = \chi_{zxx} = \tfrac{1}{2}(\cos\theta - \cos^3\theta)(\beta_{ccc} - \beta_{aac}), \tag{10}$$

$$\chi_{ZZZ} = \cos^3\theta(\beta_{ccc} - \beta_{aac}) + \cos\theta\,\beta_{aac}. \tag{11}$$

For infrared sum frequency generation, the molecular $\beta_{abc} = \alpha_{ab}\mu_c$, where α_{ab} is the Raman cross-section and μ_c is the infrared dipole transition moment for the vibration under consideration. It should be noted that there are other, non-resonant contributions to the hyperpolarizability. For metal substrates, these can be large resulting in constructive and destructive interference with the resonances. However, for dielectric substrates such as water, the non-resonant background is generally small.

Referring to equations (2) and (3), the SFG signal is thus proportional to the square of the number of molecules contributing to the signal and to their average orientation.

$$\text{Signal} \propto P^2 \propto \left|\chi^{(2)}\right|^2 = N^2\left|\langle\beta\rangle\right|^2. \tag{12}$$

Both parameters, number and orientation, must be considered when drawing conclusions about surface structure or partitioning.

2.2. *Experimental considerations*

2.2.1. *Optical line*

The experimental set-up consists of incident infrared and visible beams. These are usually pulsed lasers, often a YAG or Ti:sapphire laser with pulses ranging

Downloaded At: 16:53 21 January 2011

from ~10 ns to a few ps duration. The pulsed infrared is most often produced in an OPO/OPA (optical parametric oscillator/amplifier) although Raman shifting has also been used [42–45]. The set-up in our laboratory, shown in figure 2, consists of a Spectra-Physics GCR150 YAG laser which pumps a LaserVision KTP-based OPO/OPA to generate a 5 ns pulse of infrared tunable from 2.5–4 μm. It is the recent availability of OPO/OPA technology for production of the pulsed infrared which has enabled blossoming of this field. The infrared and visible beams are combined on the surface in copropagating geometry at 46° (IR) and 52° (visible). (Counter propagating geometry may also be used with greater dispersion for the generated sum frequency.) The infrared bandwidth is 4 cm^{-1} and the energy is 0.4–5.0 mJ/pulse. The visible, 532 nm, beam energy density is 400 mJ cm^{-2}, infrared is 100 mJ cm^{-2}.

Since the sum frequency intensity is proportional the infrared intensity which varies with wavelength, it is essential that the signal be normalized to the infrared intensity or a reference SFG signal from a surface lacking resonances. To avoid polarization-dependent loss prior to and after the cell, the sample cell in our laboratory has been designed so that the incoming and outgoing beams are perpendicular to the windows. Loss of infrared between the entrance window and the sample is measured in a simultaneous head-space measurement and all signals are normalized to the infrared intensity reaching the surface. To account for longer term variation in the pump laser, all spectra are referenced to the SFG signal of pure water at 3700 cm^{-1} for resonances between 3000 and 4000 cm^{-1} while the OD stretch of D_2O is used between 2500 and 3000 cm^{-1}. Referencing and normalization are essential for comparison of spectra.

Downloaded At: 16:53 21 January 2011

2.2.2. *Sample preparation*

Particularly for water samples, the other major experimental considerations are sample and cell preparation. The cells used in our laboratory are completely sealed with vacuum stopcocks such that only glass or Teflon® contacts the sample. Windows are sealed onto the cell with flanges and Teflon® coated o-rings. These materials provide both a good seal with temperature cycling and an inert surface to avoid sample contamination. A well-sealed cell is extremely important since contaminants often tend to partition to the surface. The cell is subjected to a 24 h soak in concentrated sulphuric–dichromate. After the soak, the cell is thoroughly flushed with 18 MΩcm nanopure water, soaked in nanopure water for an additional 24 h, and flushed again. Finally, the cell is evacuated and filled with dry nitrogen prior to introduction of the sample. The sample is introduced via a Teflon® line and transferred with ultra-high-purity nitrogen.

Water is 18 MΩcm from a Barnstead/Thermoline NANOpure® Infinity UV system. 18 MΩcm water from other sources produces equivalent spectra. In addition to conductivity, water is checked for organic impurities. One of the most reliable measures for this test is checking the 2800–3000 cm^{-1} region for C–H resonances. Since organic impurities partition to the surface and C–H resonances have good SFG cross-sections, this insures that organic impurities do not exceed more than a few per cent of a monolayer.

Salt samples sometimes have insoluble particulates from preparation filtering. Thus, most salt samples were prepared by special order of saturated solutions from GFS Chemicals® and also by neutralization of the corresponding acid with the desired alkali hydroxide. Spectra were independent of sample preparation.

3. Water orientation with subsurface ions

The primary focus of the SFG results from our laboratory is on water at the liquid–vapour interface, particularly changes in that structure upon solution formation with miscible or soluble materials. The results can be divided into two groups: those involving inorganic ions and those examining small, soluble molecules. The former includes the acids H_2SO_4 [4, 6], HNO_3 [5], and HCl [9, 46] and the salts Li, K and Cs sulphate and bisulphate, NaCl and $NaNO_3$ [6, 7, 8]. The small soluble molecules include glycerol [14], sulphuric acid [4, 6, 11] and ammonia [10, 12, 13]. Inorganic ion results and the electric double-layer model developed to understand them are contained in this section. The following section discusses soluble molecules.

3.1. *The water spectrum*

The structure of interfacial water on neat water is the foundation for this discussion. The SFG spectrum of neat water is shown in figure 1. As indicated above, the relatively narrow resonance at 3700 cm^{-1} is due to an OH bond free of hydrogen bonding. Since it is free of hydrogen bonding, it must be in the first monolayer where it accounts for an estimated 20% of the monolayer [27]. The broad peaks from 3000–3550 cm^{-1} constitute the hydrogen-bonded region. There are at least four resonances which contribute to this region: the symmetric and antisymmetric stretches of water in a symmetric environment, vibrations of water in an asymmetric environment, and the bend overtone as well as collective combinations of these modes. Since water is dynamic in its liquid temperature range, molecules are continuously exchanging between environments. Dynamics, the weakness of the hydrogen bond, and collective modes contribute to the width of the peaks. Thus, it is somewhat surprising that the hydrogen-bonded region has any structure. Interpretation of the structure is neither straightforward, nor without controversy [47, 48, 49, 50, 51, 52, 53, 54, 55]. The interpretation adopted by our group and others is based on infrared and Raman spectra of liquid water, solutions and ice [52, 53, 56]. The lower energy peak, centred near 3150 cm^{-1}, is attributed to the symmetric stretch of water in a symmetric environment. The Raman spectrum of ice in this region is more intense than in water and the depolarization ratio indicates that it is a symmetric mode [52, 53]. The remaining peak is a convolution of the other three resonances and is often referred to as the peak due to asymmetrically bonded water.

Due to the importance of water, spectral assignments in the hydrogen bonded region are a subject of intense current interest. While a survey of this field is beyond the scope of this review, two combined experimental–theoretical approaches seem to be very promising in yielding more specific information than the above skeletal description. The first is the study of related ice surfaces by Buch and co-workers [57, 58, 59]. Three coordinate water at the ice surface consists of both free-OH water and molecules with a dangling lone pair. Of the former, the hydrogen bonded OH is a local oscillator which contributes to the low frequency peak. The frequency of this feature in liquid water is very sensitive to the strength of the hydrogen bond it forms, but may also contribute to the low frequency mode in water [60]. The other studies consist of the spectroscopy of small water clusters [61]. Many features of the larger clusters, e.g. the dip just above 3200 cm^{-1} [62], resemble SFG of the surface. Interpretation of the hydrogen-bonded region in water will undoubtedly evolve as these and other studies progress. The common theme at this

Downloaded At: 16:53 21 January 2011

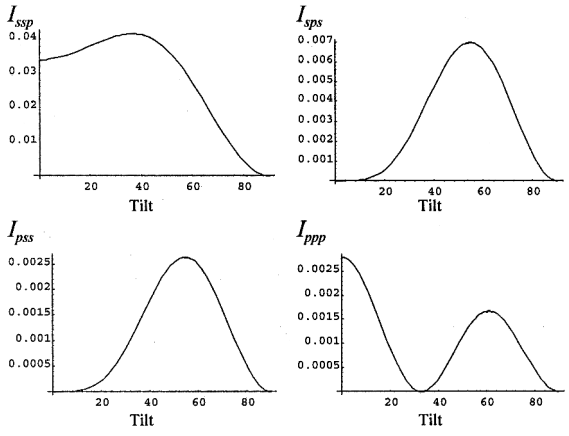

Figure 3. Free-OH intensity as a function of tilt.

Downloaded At: 16:53 21 January 2011

stage is that the low frequency peak is primarily due to relatively symmetric motions [60].

All studies concur that the free OH peak occurs only at the surface. It thus serves as a clear probe for perturbation of the top monolayer by added materials. Within the experimental bandwidth, this peak does not appear to shift or broaden, but merely decreases intensity with the addition of solutes. If the orientation is constant, a decreased intensity indicates a reduced number of free-OH water molecules. The assumption that the orientation is constant is tested with a polarization experiment as follows. For any given polarization combination, the intensity is a function of the OH tilt angle as shown in figure 3. For all angles, I_{ssp} is the most intense. However, the intensity of other combinations can be significant. For example, if interaction with a solute tilts the free OH closer to the surface, I_{sps} could be as large as 20% of I_{ssp}. Such a tilt is also expected to broaden and red-shift the resonance due to interaction with the surface. Conversely, an orientation more perpendicular to the surface orientation results in intensity for the ppp combination. Since the polarization characteristics of the free-OH peak do not change, the intensity of this peak is an indicator of the degree of perturbation of the top-most monolayer.

With the free-OH peak as a probe of surface monolayer perturbation, intensity variation in the hydrogen-bonded, 3150 cm^{-1} peak is revealing. It is reasonable to assume that if free-OH water molecules are not perturbed, i.e. the free-OH intensity is undiminished, then hydrogen-bonded water molecules in the top monolayer are also not perturbed. Therefore, an increase of intensity in the 3150 cm^{-1} peak implies that the subsequent layers of water below the top monolayer, but within the surface skin, must be perturbed. Since SFG probes all molecules within the coherence length that have a net orientation, and the coherence length is on the order of the wavelength, any perturbation which orients molecules within a thicker surface skin results in alteration of the intensity in the 3150 cm^{-1} region. Resolution concerning the question of how deep the orientation extends and the details of that orientation await further experiments. Thus, at the present time, convolution of results from the free-OH plus the hydrogen-bonded region generates a qualitative picture of water on solution surfaces.

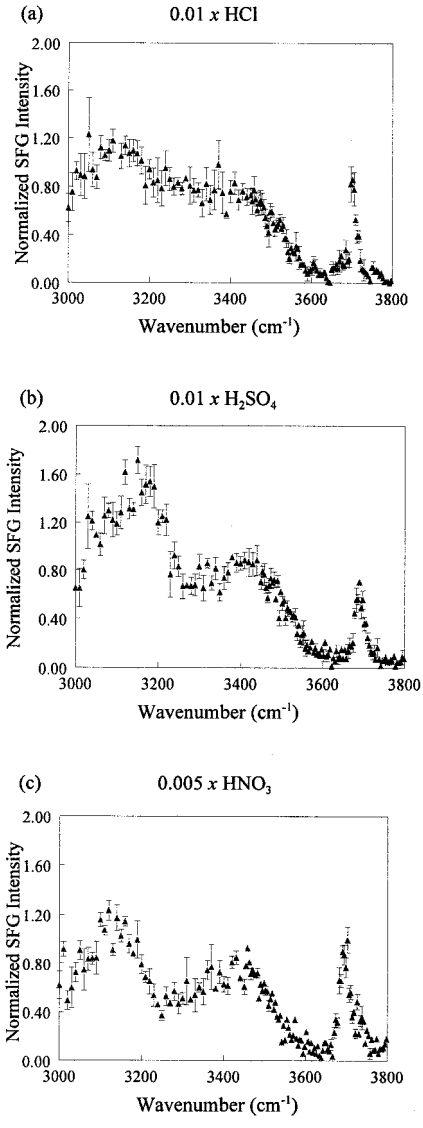

Figure 4. SFG spectrum acidic aqueous solutions: (*a*) 0.01*x* HCl, (*b*) 0.01*x* H_2SO_4 and (*c*) 0.005*x* HNO_3. Polarization: ssp.

3.2. *Results*

Consistent with the emphasis on substances which partition to the aqueous surface, previous studies addressing the orientation of surface water in the presence of charged species have focused on charged surfactants [18, 63, 64, 65]. Surfactants completely suppress the free-OH region of water since the OH is only free in the top monolayer. The orientational effect of charges near the interface are therefore detected by the effect on the hydrogen-bonded region of water. The results are consistent with anionic and cationic surfactants producing opposite interference with the low energy wing of the hydrogen-bonded region of water.

In contrast, the work in our laboratory has focused on the influence of very soluble, inorganic ions on the structure of water at the surface. Since the ions

Downloaded At: 16:53 21 January 2011

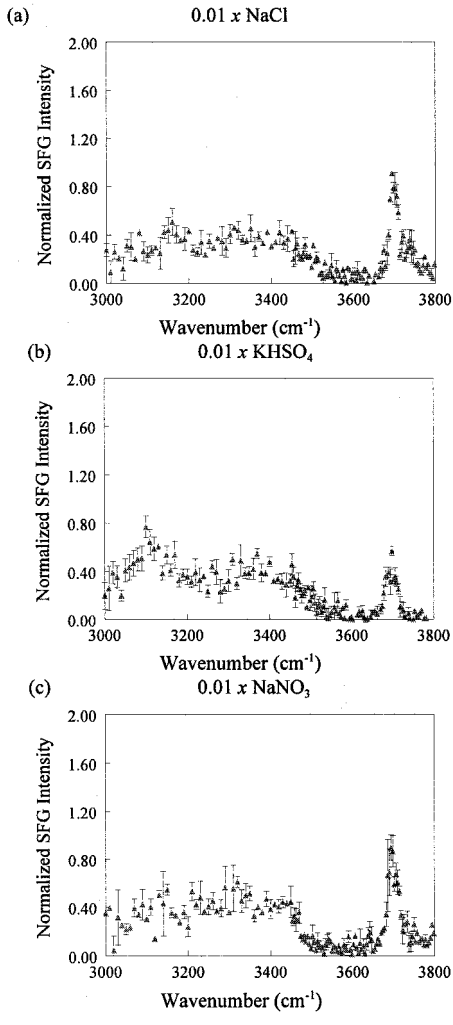

Figure 5. SFG spectrum aqueous salt solutions. Polarization: ssp.

lack a hydrophobic moiety and charges at the surface are energetically disfavoured relative to those with an intact hydration shell in the bulk, these ions are not expected to have much presence in the surface monolayer. They do, none-the-less, perturb the structure of water. Furthermore, acids perturb this structure more than the corresponding salts. The spectra of several acids are shown in figure 4 and companion alkali salts in figure 5. The free-OH peak is within experimental error of the intensity for the neat water surface. (Note: At $0.01x$ H_2SO_4, the free OH is slightly diminished.) The structure of the hydrogen-bonded region, however, is altered considerably.

These spectra demonstrate definitively that the presence of ions in solution influences the structure of water in the interfacial layer. Two sets of experiments investigate this structural change. The first examines the effect of salts—alkali sulphate and bisulphate. The spectra are shown in figure 6. Notice that the free-OH peak is diminished for every salt, although reduction in $LiHSO_4$ is marginally

Downloaded At: 16:53 21 January 2011

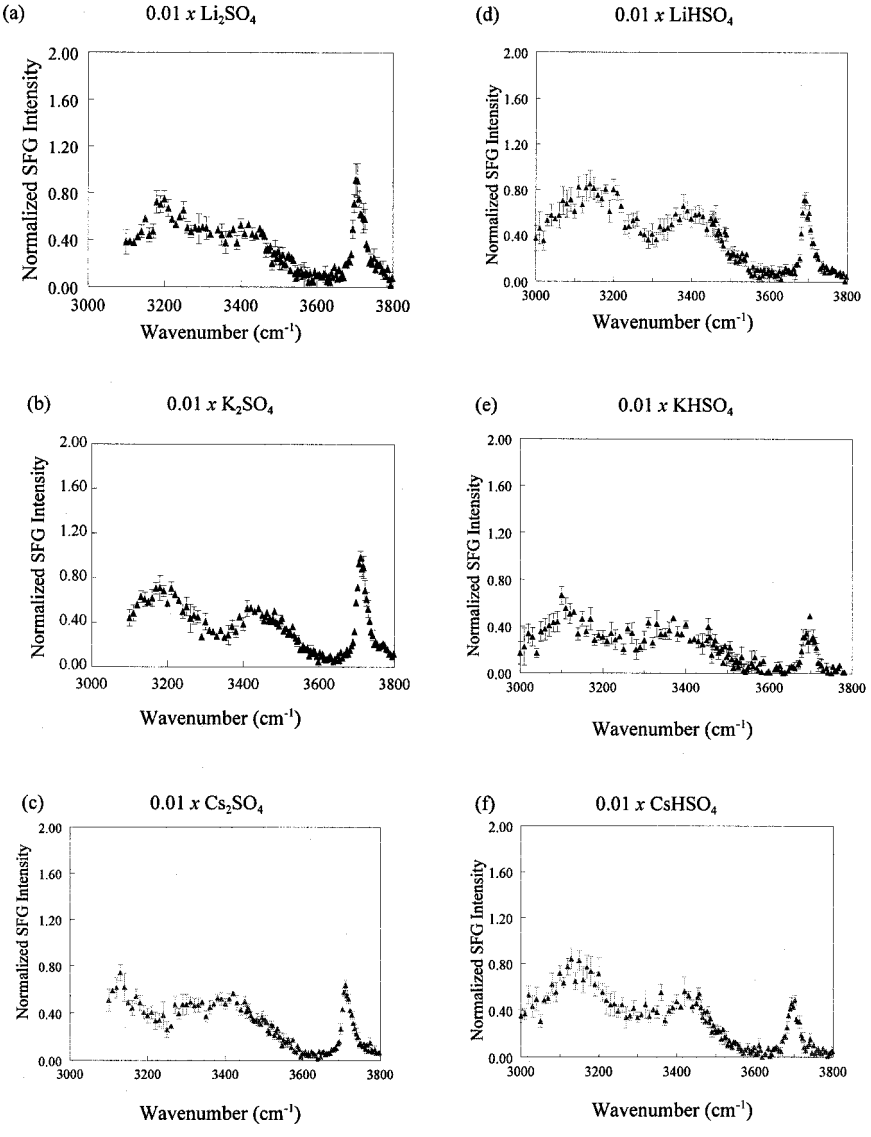

Figure 6. SFG water on aqueous salt solutions: (*a*) Li_2SO_4, (*b*) K_2SO_4, (*c*) Cs_2SO_4, (*d*) $LiHSO_4$, (*e*) $KHSO_4$ and (*f*) $CsHSO_4$. Polarization: ssp.

significant. Note that $LiHSO_4$ also shows an enhancement of the 3150 cm^{-1} peak. This point is revisited in the discussion section. In the second set, the concentration of the acid solutions is varied. The results for nitric acid are shown in figure 7. Sulphuric and hydrochloric acids show similar results [4, 9]. Decreased intensity in the 3700 cm^{-1}, free-OH peak indicates that at the higher concentrations, all three acids displace free water from the surface layer.

3.3. *Discussion*

The expectation that the extra stability associated with an intact hydration shell results in ions being in the bulk rather than on the surface is confirmed by the undiminished free-OH intensity in the spectra in figures 4 and 5. Surface tension

Downloaded At: 16:53 21 January 2011

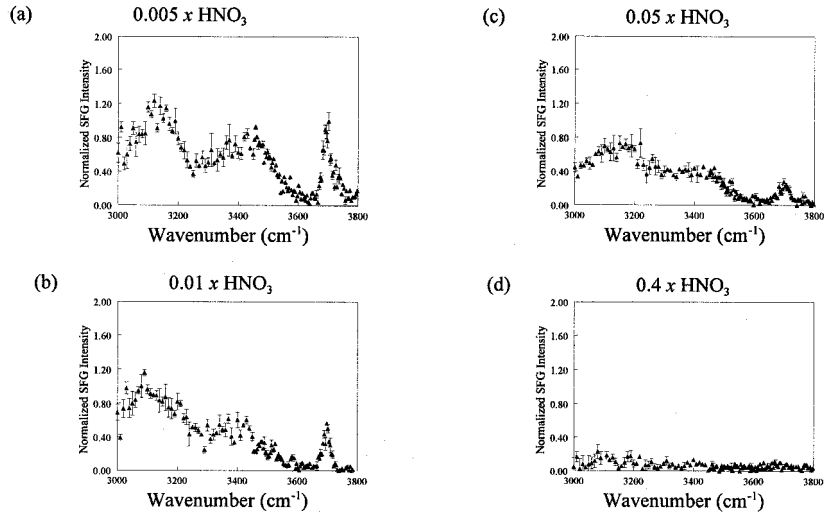

Figure 7. SFG spectra of aqueous nitric acid solutions: (*a*) 0.005*x*, (*b*) 0.01*x*, (*c*) 0.05*x* and (*d*) 0.4*x*. Polarization: ssp.

Downloaded At: 16:53 21 January 2011

results [66, 67, 68, 69, 70] also predict a shortage of ions and an excess of water at the interface, so this result is not surprising. What is unexpected is the change in structure of water at the interface particularly for the acids. These results suggest that ions penetrate to *near* the interface.

Several studies have been conducted to understand the nature of the air–electrolyte solution interface which support models of ions at least approaching near to the interface. Early work of Onsager and Samaras on the surface tension of electrolyte solutions indicates that ions approach to within 3×10^{-8} cm of the interface [71]. This early work is supported by a recent study of the free energy of ions approaching a curved interface [72] and by molecular dynamics calculations and ultraviolet photoemission spectroscopy (UPS) experiments which have shown that Cs^+ ions specifically approach to within 3.75 Å of the air interface in an $x > 0.2$ CsF solution [73]. In infinitely dilute solution, molecular dynamics calculations indicate ions approach the surface with their solvation shells intact [74]. In all these investigations, the air–liquid interface contains at least 1–2 layers of water. The SFG results presented here are consistent with these earlier results while providing a more detailed molecular picture.

3.3.1. *The double layer model*

Probably the most noticeable feature of the spectra in figure 4 is the large intensity in the hydrogen-bonded region, particularly the peak at 3150 cm^{-1}. It is tempting to assign this large peak to H_3O^+. However there are several reasons to believe that this is not the correct assignment. (1) In HCl solutions it has been suggested that H_3O^+ is at the surface and oriented with the dipole perpendicular to the interface [75]. The hydronium ion OH stretches have been variously assigned to 3170 cm^{-1} [76], 2800 cm^{-1} [77], 2670 cm^{-1} [77], or as low as 2550 cm^{-1} [78]. The only reference to assign a band as high as 3170 cm^{-1} to H_3O^+ assigns it to the *antisymmetric* stretch of H_3O^+. If H_3O^+ is oriented with OH bonds toward the bulk liquid, a reasonable orientation given stabilization of the positive charge by

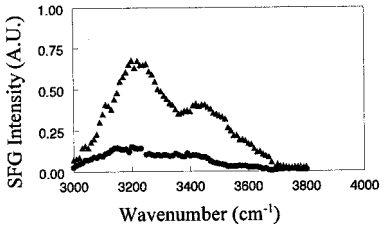

Figure 8. SFG spectrum of water at a quartz interface: ● = pH = 2; ▲ = pH = 12. Polarization: ssp, temperature = 294 K.

greater hydration in this orientation, then the antisymmetric vibrational dipole is perpendicular to the surface normal. A dipole perpendicular to the normal cannot be detected in ssp polarization, thus it cannot contribute to the 3150 cm^{-1} band. (2) Assignment at 3150 cm^{-1} is probably too high since hydrogen-bonded H_3O^+ bands are expected to be significantly red-shifted relative to water (< 3000 cm^{-1}) [79]. (3) At these acid concentrations the predominant solution species is expected to be $H_5O_2^+$ which absorbs below 3000 cm^{-1} [79, 80]. No evidence for bands below 3000 cm^{-1} have been observed in the interface [46]. (4) The free-OH band is not perturbed. The H_3O^+ resonance would have to be extremely intense to enhance the 3150 cm^{-1} band, yet have low enough concentration to leave the free OH unperturbed. Hence, the 3150 cm^{-1} band is assigned to hydrogen-bonded water.

An electric double-layer model involving ions near the interface is used to understand the increased intensity in the hydrogen-bonded region. Although ions approach the interface, the distribution of anions and cations is not identical. Experiments and calculations have determined a tendency for anions to partition to the surface over cations. In dilute solutions, molecular dynamics calculations indicate that Cl^- and F^- anions penetrate closer to the air–liquid surface than cations [74, 81]. Surface potential experiments involving inorganic electrolyte solutions confirm that the negative ion penetrates closer to the interface [82].

This preferential partitioning of the anion closer to the surface is understood as due to its more polarizable nature, larger size, lower hydration energy, and lower hydration number compared to the cation [66, 74, 83, 84]. The broken isotropic symmetry at the air–solution interface necessarily leads to less water for solvation of ions, thus favouring anions over cations. This differential ion distribution creates an electric double layer just beneath the surface. Water molecules respond to the excess negative charge at the surface by orienting with hydrogen atoms pointing further into the bulk solution. This re-orientation of surface and sub-surface water molecules, relative to neat water, leads to an increased SFG signal both because the dipole moment of H_2O is more perpendicular to the interface and because more layers are oriented. This effect is also observed for water at a negatively charged quartz–water interface. The SFG spectrum of this interface, shown in figure 8, is in good agreement with that of Shen and co-workers [85]. At low pH, the quartz surface is neutral and the intensity is only about 1/4 that of the basic pH case in which the surface is negatively charged. (Note that at the solid interface, there is no free OH.)

The spectrum of the hydrogen-bonded region of 0.01x H_2SO_4, figure 4, closely resembles the basic pH quartz–water spectrum: the intensity of 0.01x H_2SO_4 is five

Downloaded At: 16:53 21 January 2011

times that of water between 3000–3300 cm^{-1}. Although not quite as dramatic, the other acids, HCl and HNO_3, also significantly increase the intensity of the 3150 cm^{-1} peak. The greater influence of acids on the intensity of this peak compared to that of the 0.01x salt solutions is striking. This larger intensity for the acid solutions is attributed to a more extensive double layer formed by the acids due to less effective neutralization of the anion charge by H^+ compared to Na^+ and K^+—H^+ cannot approach as close to the negative ions as the metal ions because of its effective size. The insensitivity of the 3000–3300 cm^{-1} peak to the different metal cations [7] is due to their nearly equal effective radii (Stokes radii) in solution [84]. The similar effective radii leads to ions creating a double-layer structure of comparable thickness, resulting in electric fields of similar strength. The spectra in figures 4 and 5 suggest that bisulphate (the primary negative ion in 0.01x sulphuric acid) enhances the double layer more than nitrate or chloride. This is reasonable given the smaller size of the nitrate and chloride ions.

3.3.1.1. *Solvated ions and associated complexes* . In concentrated solutions, there is a high degree of association among the ions. Associated ions are charge-neutral, can penetrate to the surface, and interfacial water bind directly to the complex.

$$
\begin{array}{l}
1\ \boxed{2\ M^+(aq)\ +\ SO_4^{2-}(aq)} \\
\qquad \uparrow\downarrow K_{association} \\
2\ \boxed{\begin{array}{ccccc}
M^+(aq) & + & MSO_4^-(aq) & \rightleftharpoons & M_2SO_4(aq) \\
 & & \uparrow\downarrow & & \uparrow\downarrow \\
M^+(aq) & + & M^+SO_4^{2-}(aq) & \rightleftharpoons & (M^+)_2SO_4^{2-}(aq)
\end{array}} \rightleftharpoons \begin{array}{c} M_2SO_4(s)\ \text{or} \\ H_2SO_4(aq) \end{array}
\end{array}
\qquad (13)
$$

An example of the species in solution is shown in (13). The species in box 1 are solvated ions, and the species in box 2 are associated species such as contact-ion pairs or hydrated complexes. The relative concentration of associated and solvated species is determined by the association constant, $K_{association}$. At low salt concentrations, solvated ions are the predominant species in solution. For example, the primary solvated species in 0.01x solutions are M^+ (M = Li and K) and SO_4^{2-} [86–88]. As concentration increases, the degree of association increases in accord with the hard/soft character of the ions involved [89]. For group IA metals, the degree of soft character increases as the group is descended in the periodic table [66, 84, 87, 90, 91]. Since sulphate and bisulphate anions are relatively soft [92], the degree of association increases from Li^+ to Cs^+. Accordingly, the spectra in figure 6 reveal that the free OH is only slightly diminished for $LiHSO_4$ while that for $KHSO_4$ and $CsHSO_4$ are comparably reduced. Similarly, for both Cs^+ and K^+, the bisulphate salts diminish the free OH more than the corresponding sulphate salts, figures 5 and 6. Bisulphate is singly charged making it softer than sulphate. As salt solutions become more concentrated, the associated ions precipitate.

An increase in the concentration of the solute shifts the equilibrium from solvated ions to hydrated ion-pair complex formation. For a very soluble electrolyte, this eventually leads to nearly all the ions being associated with each other leaving no free ions available to form an electric double layer. The molecular species thus formed, can displace water or bind it into a hydrated complex. This is the case for nitric and sulphuric acid solutions. As the concentration of HNO_3 increases above 0.005x, the 3000–3300 cm^{-1} peak decreases and goes to zero at 0.4x HNO_3

Downloaded At: 16:53 21 January 2011

(figure 7). For a substance with limited solubility, such as the salts, there are always ions in solution to participate in a double layer structure at the air–liquid interface. The decrease of the 3000–3300 cm^{-1} peak for the salts is limited by the solubility of the compound.

Recapping the results for ionic solutes:

(i) At very low concentration, the stability of ions in the bulk relative to those at the surface leaves surface water unperturbed.

(ii) As solute concentration is raised, ions approach nearer to the interface. However, the distribution of anions and cations are not identical—the tail of the anion distribution extends slightly closer to the surface than that of the cations. This differential distribution results in an electric double layer. Water molecules in the surface respond to this electric field by tilting with the dipole slightly more toward the normal. At this concentration, $\sim 0.01x$ for the salts and acids investigated, the top-most monolayer remains unperturbed. These changes are reflected in the SFG spectrum: the free-OH intensity is unchanged while the hydrogen-bonded peaks, particularly the symmetric peak, increase significantly.

(iii) At yet higher concentration, the population of associated ion complexes and molecular species becomes significant. At these concentrations, acids and salts diverge a bit. Salts reach the solubility limit and precipitate. If the cation is sufficiently large, the associated ions can incorporate surface water into the hydration shell and eliminate the free OH [6, 7]. Acids, like salts with large cations, form associated ion complexes or molecular species. As ions associate, the stronger acid double layer is diminished due to charge neutralization and the intense hydrogen-bonded peaks diminish.

(iv) Since acids do not precipitate, the concentration can be increased yet further. Surface water is incorporated into the hydration shell diminishing both the free-OH and hydrogen-bonded intensity. Note that the very volatile acid, HCl, never reaches the point of displacing surface water since molecular HCl desorbs readily [46].

Downloaded At: 16:53 21 January 2011

4. Molecular solutes

Molecular solute here refers to a material that is miscible with water or which is primarily molecular. Sulphuric acid and glycerol fall into the first category while ammonia falls into the second. Sulphuric acid is a strongly hydrogen-bonding molecule which forms a very non-ideal solution with water. In contrast, glycerol forms a nearly ideal solution yet evidence indicates that both of these significantly alter water at the interface. In particular, at 20 mole% glycerol completely covers the surface. Ammonia has often been used as a probe molecule for solid surfaces. Surface tension data suggests that ammonia forms a stable surface complex with water. SFG provides the tool to investigate the structure of this complex. Each of these systems is discussed below.

4.1. *Sulphuric acid*

The structure of water on the surface of aqueous sulphuric acid solutions is typical of acidic solutions, discussed in the previous section. The focus of this section is on the free-OH peak. This peak is a probe for perturbation of the first monolayer. To make this measure quantitative, the intensity of the free-OH peak for each concentration is referenced to the free OH of the neat water interface. Plotting

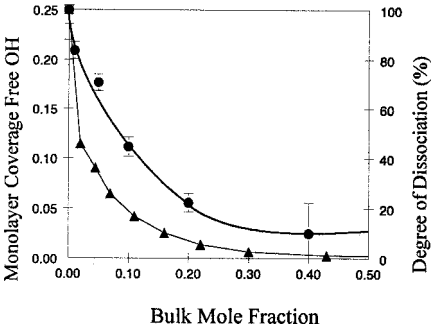

Figure 9. Monolayer coverage free OH and degree of dissociation versus mole fraction: degree of dissociation [93] (▲); free OH of water from SFG data (●).

the square root of this ratio (since the SFG intensity is proportional to the square of the number of molecules contributing to the signal) measures unperturbed water at the surface. For sulphuric acid, this ratio is shown in figure 9. Since a sulphuric acid molecule occupies about three times the area of a water molecule, the area fraction decreases more rapidly than the mole fraction. However, examination of the data in figure 9 indicates that the signal from water decreases even more rapidly than expected from mere truncation of the bulk. For example, at 10 mole% acid, truncation would result in a surface area coverage of 75% for water. The data in figure 9, however, reveal that water has fallen to about half. The conclusion is that surface water is perturbed beyond mere random mixing.

Sulphuric acid is a major industrial chemical. In addition, heterogeneous surfaces in the stratosphere are sulphate solutions and these surfaces catalyse destruction of ozone. Thus, the composition of the surface of sulphate solutions is of interest. Calculations [94], Auger electron spectroscopy (AES) and X-ray photoelectron spectroscopy (XPS) experiments [95] indicate that the composition (sulphuric acid/water ratio) of the surface and that of the bulk are the same. Since unperturbed water, as measured by the SFG free-OH signal, is diminished, part of the water must be bound in hydrates with molecular sulphuric acid. Correlation between perturbation of the free-OH intensity and the degree of association, shown in figure 9, is consistent with the picture of molecular sulphuric acid penetrating to the surface and binding adjacent water molecules.

An alternate interpretation of the sulphuric acid spectra has been presented by Radüge *et al.* [96]. At low concentration, $< 0.1x$, the hydrogen-bonding nature of sulphuric acid is emphasized. At higher concentration, the disappearance of water resonances is attributed to the crystalline structure of water–sulphuric acid. Due to the high degree of dissociation at low concentration and the very similar picture presented by other acids, HNO_3 and HCl, we favour the ionic picture at low concentrations. At higher concentrations, these acids also diminish the signal from water.

For heterogeneous stratospheric chemistry, the tetrahydrate (SAT, 58 wt%, $0.2x$) is of particular interest. At stratospheric temperatures (205–240 K), $H_2SO_4 \cdot 4H_2O$ may be either a crystalline solid or a supercooled liquid. In either case, bulk measurement indicate that sulphuric acid becomes increasingly ionic as the temperature is lowered [97, 98]. The important question for understanding stratospheric chemistry is, what is the structure of water on these surfaces? At 0°C, $0.2x$ sulphuric

Downloaded At: 16:53 21 January 2011

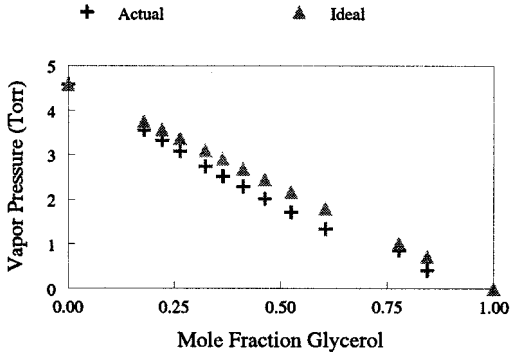

Figure 10. Water vapour pressure versus mole fraction glycerol: experimental [99] (+); Raoult's law (▲).

acid shows no free-OH resonance and the signal from hydrogen-bonded water is small. If the solution becomes increasingly ionic as the temperature is lowered, the hydrogen-bonded region should increase intensity. If the surface is covered with water, a free-OH peak may also appear. Thus, a $0.2x$ sulphuric acid solution was supercooled to 216 K and the surface examined. The spectrum is indistinguishable from that at 0°C [11]. The conclusion is that the surface not only is not covered with water, but the increased degree of dissociation in the bulk is not reflected at the surface. This issue is currently under further investigation.

4.2. *Glycerol*

In contrast to sulphuric acid and water, glycerol and water form a nearly ideal solution. Figure 10 shows the plot of vapour pressure versus mole fraction. Note that the vapour pressure of glycerol is essentially zero. However, since the surface tension of glycerol is lower than that of water, the system energy is lowered if glycerol is in excess at the surface. Indeed, surface tension measurements [99] indicate an excess of glycerol at the surface. The glycerol CH resonances are well separated from those of water, thus glycerol at the surface can be quantified with SFG: as long as the orientation remains the same, the square root of the SFG intensity is proportional to the surface concentration. Since pure glycerol has a surface mole fraction of one, the monolayer coverage with glycerol can be measured and coverage for solutions determined.

Resolution of the orientation issue for glycerol is as follows. As indicated in figure 11, there are two CH resonances: the symmetric and antisymmetric CH stretches at 2880 cm^{-1} and 2945 cm^{-1} respectively. Since the dipole for these two are orthogonal, if the intensity ratio of the two resonances is constant, the orientation must also be constant. This is the case for solutions with $x > 0.07$ [14]. Thus, referencing all intensities to the pure glycerol surface enables determination of the surface mole fraction. The data is shown in figure 11 and the surface coverage in figure 12. A similar referencing to the neat water surface determines the surface coverage in monolayers for free-OH water. Assuming that unperturbed water maintains the same free-OH to hydrogen-bonded population ratio, this estimates the hydrogen-bonded coverage. (Note: Measurement of the intensity in the hydrogen-bonded region cannot be used since both glycerol and water have OH resonances

Downloaded At: 16:53 21 January 2011

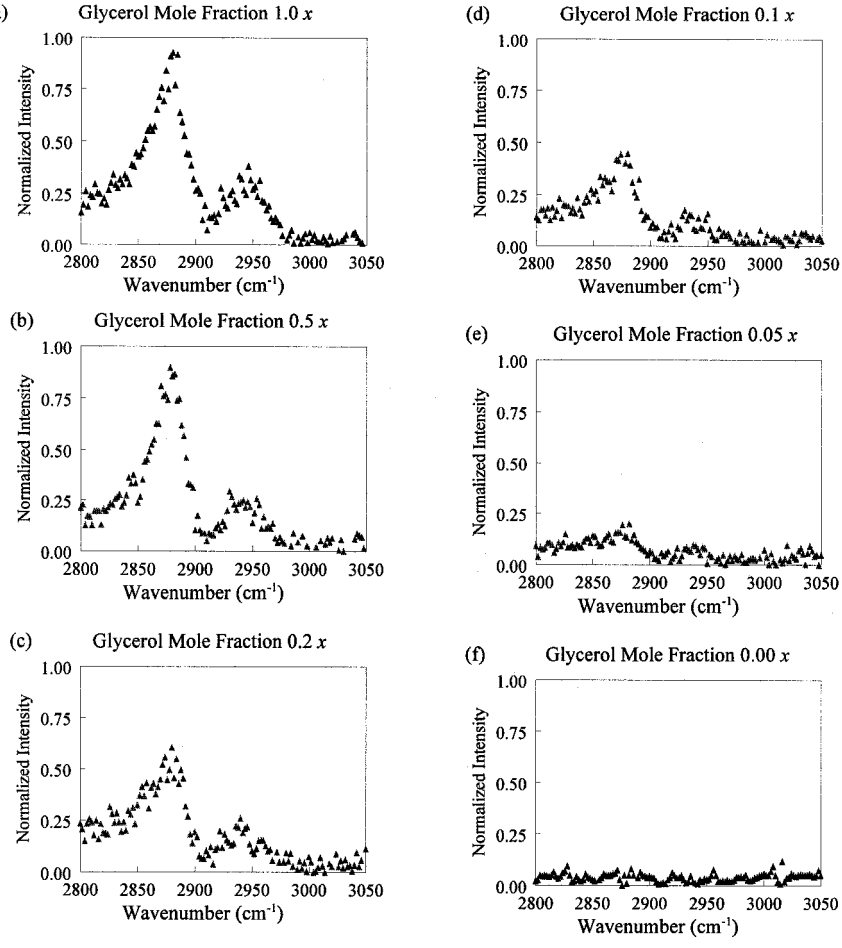

Downloaded At: 16:53 21 January 2011

Figure 11. SFG of the CH region of glycerol. Polarization: ssp.

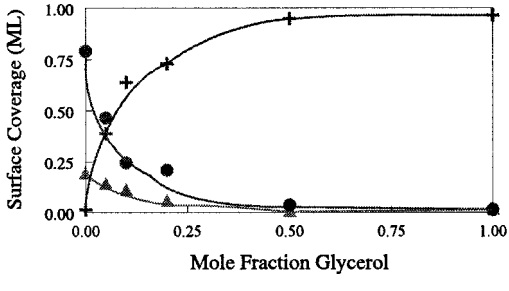

Figure 12. Surface coverage versus bulk mole fraction glycerol: glycerol (+), hydrogen-bonded water (•) and free OH (▲).

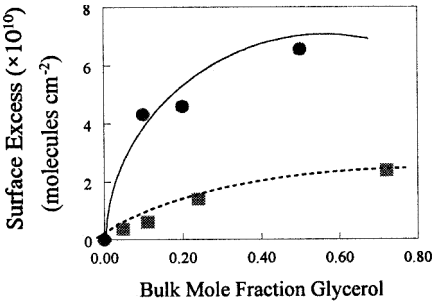

Figure 13. Surface excess glycerol versus bulk mole fraction glycerol: SFG data (●) and surface tension data (■).

in this region.) The surface coverage in monolayers (ML) for both types of water are also shown in figure 12. Note that the total coverage is 100% validating the assumption about hydrogen-bonded and free-OH water. Thus SFG has determined all molecules on the surface of this mixture.

Conversion from monolayer coverage to surface mole fraction utilizing the area occupied by each [100] determines the surface excess of glycerol. The surface excess is the actual number of molecules per square centimetre compared to the number expected from truncation of the bulk. Like surface tension, SFG data indicates that glycerol is in excess at the surface. Importantly, as indicated in figure 13, SFG data indicates an even larger surface excess than surface tension data. This difference is attributed to the different depths measured by the two techniques. Surface tension is a macroscopic measurement, while SFG is sensitive to those molecules which have a net orientation. It is reasonable that if there is a gradient in glycerol concentration from the bulk value to a higher value on the surface, and if fewer layers are measured, the excess will be greater.

In sum, the picture of the surface of glycerol–water solutions is very complete. Both glycerol and water are detected directly. Calibrating with the two neat surfaces, accounts for the complete monolayer. At about 25 mole% glycerol, glycerol blankets this surface. Glycerol is hygroscopic because water at the surface is a higher energy configuration, consistent with conclusions from surface tension experiments.

4.3. *Ammonia*

The motivation for studying the interaction of ammonia with different surfaces stems from its importance in heterogeneous catalysis and its relevance to various industrial processes. The structure and adsorption characteristics of ammonia on transition metal [101–104] and metal oxide [105, 106, 107] surfaces have been studied in great detail, primarily with ultra-high vacuum techniques. The configuration of ammonia on these surfaces is well known, and trends for chemisorption and physisorption are observed for a number of surface-specific experiments. Adsorption sites differ according to the substrate; however, ammonia is generally bonded to a surface via the nitrogen atom lone pair electrons with the C_3 molecular axis perpendicular to the surface plane [103]. At high coverage, however, the molecule is commonly observed to tilt with respect to the surface normal [108].

In addition to solid substrate interactions, gas- and aqueous-phase ammonia participates in numerous atmospheric processes [109], such as aerosol formation

Downloaded At: 16:53 21 January 2011

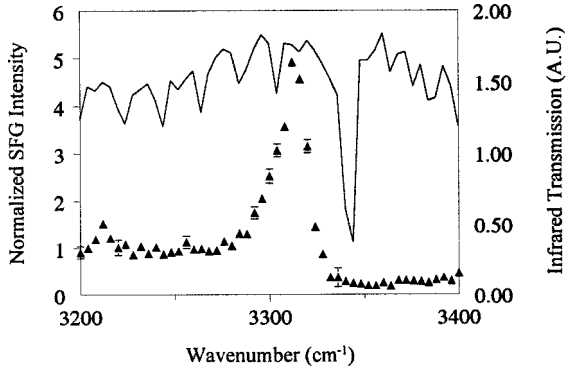

Figure 14. Ammonia: SFG spectrum concentrated ammonia relative to the free OH of neat water (▲) and gas-phase infrared spectrum (—). SFG polarization: ssp.

and NO_x reduction. Ammonia (and NH_4^+) plays a unique role in environmental chemistry as the most significant alkaline gas in the atmosphere, readily reacting with sulphuric, hydrochloric and nitric acids [110, 111]. Therefore, it is desirable to ascertain aqueous-phase structural information of ammonia molecules at liquid interfaces to determine chemical reactivity occurring on heterogeneous surfaces.

As early as 1928, Rice conjectured that ammonia forms a surface complex on water [112]. The SFG spectrum, shown in figure 14 confirms this complex. The dominant feature at $3312\,cm^{-1}$ is assigned to the ν_1 symmetric stretch of ammonia at the liquid–vapour interface. Note the large intensity relative to the free OH of neat water so that the ammonia peak dominates the spectrum. The symmetric stretch is red shifted from the gas-phase absorption by $\sim 20\,cm^{-1}$ [113]. Both the small shift and the narrow resonance indicates that interaction with the surface is weak. The smaller peak just above $3200\,cm^{-1}$ is assigned to the overtone of ν_4, the asymmetric angle deformation mode. Although not shown in figure 14, the free-OH stretch of water is completely suppressed for concentrated ammonia.

The asymmetric shape of the resonance at $3312\,cm^{-1}$ deserves special comment. It is tempting to assign this to interference between the underlying hydrogen-bonded OH resonances of water and the ammonia stretch. A similar interference has been noted for charged surfactants on water [64]. Although such an interference is probably present, it cannot account for the asymmetric shape for the following reasons. (1) The ammonia resonance is *much* more intense than that of water. The observed complete lack of signal on the blue side of the resonance requires exact cancellation of signal. (2) The Raman spectrum of aqueous ammonia [114] has a very similar shape. In the case of aqueous ammonia, the asymmetric shape is attributed to the structure of the Q band since the gas-phase Raman ν_1 band is also asymmetric. This structure due to the Q band is further evidence for the weak interaction between ammonia and water.

A significant strength of SFG is the capability to determine of the orientation of surface-adsorbed molecules. This orientation can reveal information about interactions among surface species. This is the case with ammonia. For a detailed discussion of the orientation analysis, the reader is directed to the literature [12, 13]. Briefly, two polarization combinations yield non-zero spectra: ssp and sps. These are shown in figure 15.

Downloaded At: 16:53 21 January 2011

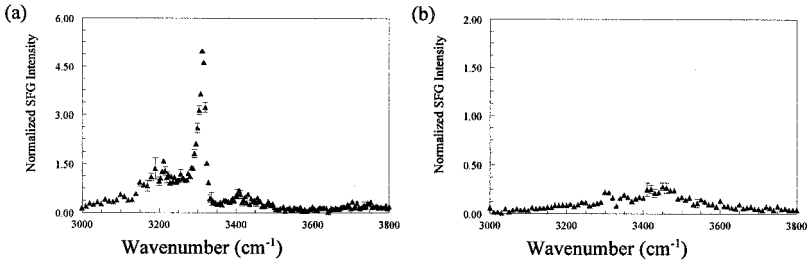

Figure 15. SFG spectra of concentrated ammonia.

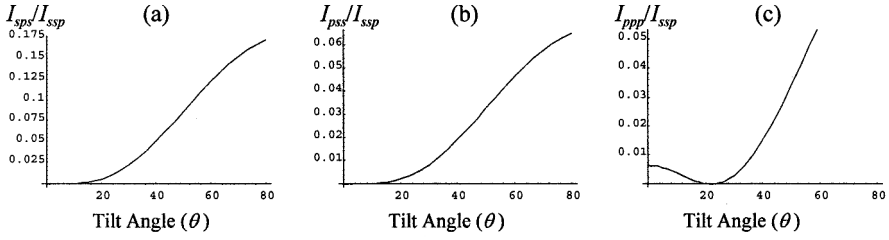

Figure 16. Intensity versus tilt angle for symmetric stretch of ammonia: (*a*) I_{sps}/I_{ssp}, (*b*) I_{pss}/I_{ssp} and (*c*) I_{ppp}/I_{ssp}.

Downloaded At: 16:53 21 January 2011

Note in particular, that the *symmetric* stretch only appears in ssp polarization. The molecular parameters needed to analyse these results include the Raman transition moments, α_{ij} and the infrared dipole moment, μ_c for the symmetric stretch. These are given by Girardet and co-workers [115]. Only three Raman transition moments are non-zero for the symmetric stretch. They are $\alpha_{AA} = \alpha_{BB} = 1.97\,\text{Å}^2$ and $\alpha_{CC} = 4.39\,\text{Å}^2$ and the infrared dipole moment is $\mu_C = 1.40\,\text{D Å}^{-1}$. Applying the rotational and Fresnel factor analysis results in the intensity ratios shown in figure 16. Zero tilt corresponds to the C_3 axis lying along the normal, perpendicular to the surface. Note particularly, the *non-zero* intensity for ppp polarization at zero tilt is about at the detection limit. Hence, from the symmetric stretch, we conclude that ammonia is tilted $\leqslant 38^\circ$ from the surface normal.

While the preceding discussion of the symmetric stretch has limited the ammonia tilt, an analysis of the doubly-degenerate, antisymmetric stretch narrows this tilt yet further. Analysis of the antisymmetric stretch is more involved than that of the symmetric stretch due to the degeneracy. In addition, the intensity is a function of both the tilt (θ) and the twist (ϕ) angles. In the analysis, the molecular normal modes, *ABC*, are projected onto the molecular Cartesian coordinate system, *abc*. The procedure is similar to projecting the surface coordinate system, *xyz*, onto the laboratory coordinate system *XYZ*. For an isotropic surface such as water, these two are related by a random rotation angle. For ammonia, there are three equivalent orientations of the molecular normal coordinates with respect to the molecular Cartesian coordinates due to the C_{3v} symmetry. The Cartesian coordinate infrared and Raman transition moments are an average over these three equivalent orientations.

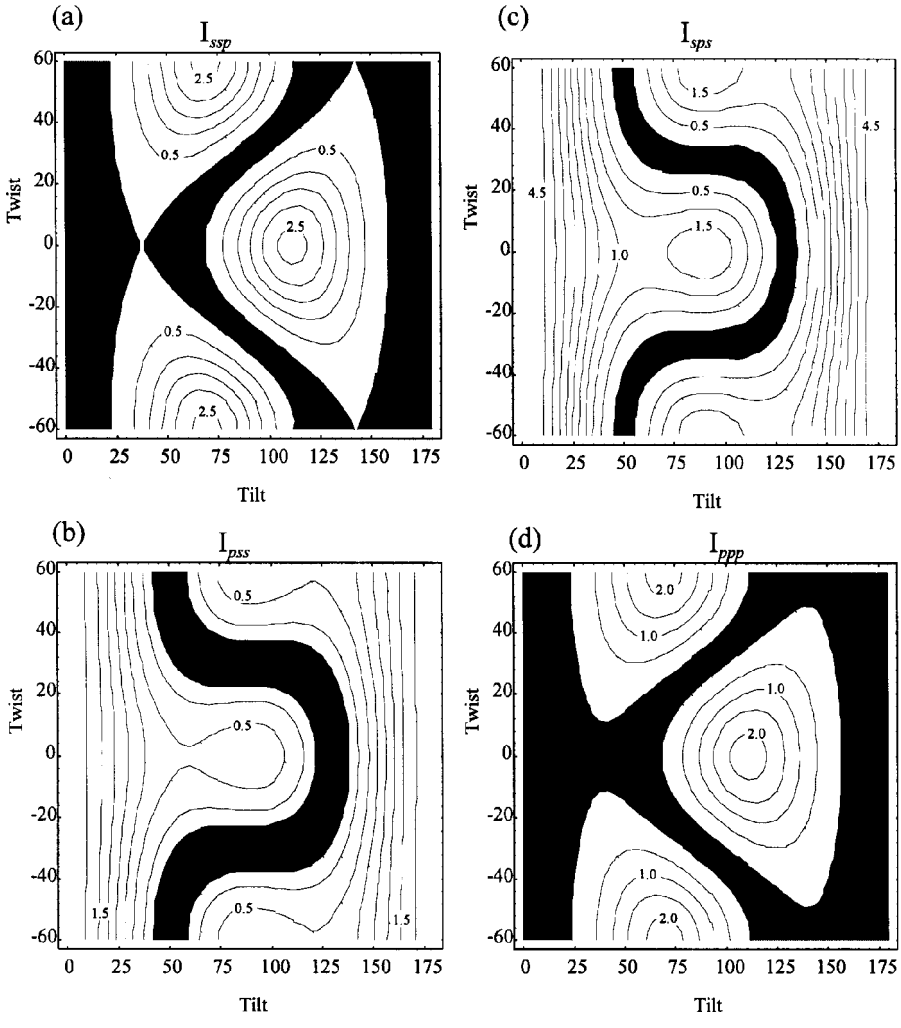

Figure 17. Contour plots of intensity versus tilt and twist angles for the antisymmetric stretch of ammonia.

Downloaded At: 16:53 21 January 2011

The normal mode infrared and Raman transition moments are [115]

Normal Mode A:

$$\left(\frac{\partial\alpha}{\partial Q_A}\right) = \begin{pmatrix} 0 & -\alpha_3 & -\alpha_2 \\ -\alpha_3 & 0 & 0 \\ -\alpha_2 & 0 & 0 \end{pmatrix} \quad \left(\frac{\partial\mu}{\partial Q_A}\right) = \begin{pmatrix} \mu_A \\ 0 \\ 0 \end{pmatrix}, \tag{14}$$

(Raman) (infrared)

Normal Mode B:

$$\left(\frac{\partial\alpha}{\partial Q_B}\right) = \begin{pmatrix} \alpha_3 & 0 & 0 \\ 0 & -\alpha_3 & \alpha_2 \\ 0 & \alpha_2 & 0 \end{pmatrix} \quad \left(\frac{\partial\mu}{\partial Q_B}\right) = \begin{pmatrix} 0 \\ \mu_B \\ 0 \end{pmatrix}. \tag{15}$$

(Raman) (infrared)

These are projected onto the Cartesian coordinate system for each of the three possible orientations to yield the non-zero hyperpolarizabilities:

$$\beta_{aaa} = -\beta_{bba} = -\beta_{bab} = -\beta_{abb} = \alpha_3(\mu_A - \mu_B)/2 = 8.42\ \text{D Å}, \tag{16}$$

and

$$\beta_{caa} = \beta_{cbb} = \beta_{aca} = \beta_{bcb} = \alpha_2(\mu_B - \mu_A) = -6.94\ \text{D Å}. \tag{17}$$

Results of analysis of the antisymmetric mode are shown in figure 17. The zero contours have been highlighted to aid in the analysis. The only polarization which shows non-zero intensity for the antisymmetric stretch is sps (figure 15). Since both ssp and ppp are zero for a large range of tilt and twist, these do not narrow the orientation results from the symmetric mode analysis. The polarization combination which limits the orientation of ammonia is pss. The pss spectrum is extremely flat, implying a tilt angle of $34° \leqslant \theta \leqslant 38°$. Preliminary results indicate that this orientation does not change as the concentration of ammonia is lowered. SFG does not provide a direct answer to the question of whether nitrogen is up or down. However the nitrogen up orientation with a tilt of $\sim 35°$ would likely lead to two N–H stretches due to stronger interaction by hydrogen closer to the surface. This issue can be definitively resolved with a phase-shift measurement.

In summation, SFG has verified the conjectured complex between ammonia and water at the aqueous surface. Further, the combined polarization and spectroscopic data determines detailed information about the structure of ammonia on the aqueous surface. The C_3 axis is tilted between 34° and 38°. As noted at the beginning, many molecules are tilted at approximately this angle on the aqueous surface.

Downloaded At: 16:53 21 January 2011

5. Summary

In summary, SFG provides a powerful, molecular-level probe of liquid interfaces. Given the dynamic nature and high vapour pressure of most liquid interfaces, SFG and the related technique, SHG, are often the only current methods available to probe these surfaces. Adoption of the technique, previously hampered by lack of high-powered, tunable, infrared pulses has blossomed following development of OPO/OPA technology. As these technologies open yet longer wavelengths, it is expected that SFG will be applied to a large variety of surfaces.

Generation of the sum frequency depends on the inherent non-isotropic nature of the surface. Utilizing an infrared and a visible frequency results in a vibrational spectrum of the surface. It is the combination of vibrational and polarization data that makes SFG particularly powerful. This review begins with an outline of the development of the technique beginning with the theoretical underpinnings in the early 1960s by Bloembergen and Pershan [15] through investigation of the neat water surface by Shen and co-workers in 1993 [27]. The work in our laboratory has focused on changes at the aqueous surface upon addition of salts, inorganic acids and miscible molecules. Thus, the foundation of this work can be traced to 1993. For atmospherically relevant chemistry as well as chemistry associated with corrosion, salts, inorganic acids and miscible molecules are highly relevant. The combined work on salts and inorganic acids is unique to our laboratory.

The results indicate that inorganic ions in solution influence the structure of water at the surface. Although surprising at first, this result is consistent with theoretical and experimental results which indicate that the distribution of the larger, more polarizable negative ion in a salt or acid extends closer to the interface than the

distribution of the cation. Based on the differential distribution of anions and cations, we have developed an electric double-layer model for these results. Briefly, water responds to the tail of the negative charge distribution by reorienting relative to neat water with the dipole more normal to the surface and with additional layers of water having a net orientation. As a broad generalization, the work shows that acids have a stronger effect on interfacial water than the corresponding salts. Due to the effective size of the proton, it has an anomalously high hydration energy. The proton distribution is therefore more separated from the negative charge distribution than other cations. This results in a more extensive electric double layer and an extreme intensity for hydrogen-bonded water.

This model is consistent with the greater hydrogen-bonded intensity for bisulphate salts than sulphate salts due to the single charge of the former and double charge of the latter. It is also consistent with a stronger orienting effect with sulphuric acid than nitric or hydrochloric: the HSO_4^- ion is larger than NO_3^- or Cl^-. As acid or salt concentration is increased yet further, associated ion complexes or molecular species penetrate to the surface monolayer and both suppress the free-OH peak and diminish the hydrogen-bonded peaks. The spectroscopy of water on these surfaces has provided rich details about ions near the interface.

Water miscible molecules have the potential for investigation of an even wider concentration range. Examining both sulphuric acid which forms a very non-ideal solution with water and glycerol which forms a nearly ideal solution, indicates that both of these hygroscopic materials partition to the surface. As a generalization, it appears that the material with the lower surface tension partitions to the interface and, at least for ideal solutions, the composition of the vapour phase is determined by the bulk, not the surface.

Ammonia is found to form a complex with water on the surface of aqueous solutions. Ammonia is often used as a probe for solid surfaces where it is usually found to be perpendicular to the surface at low concentrations and to tilt at higher concentrations. A combination of spectral and polarization analyses determines the orientation of ammonia to be tilted on the aqueous surface. Many molecules are tilted about 40° from the normal on aqueous surfaces. The tilt of ammonia, 34–38°, fits into this generalization as well. It appears that the water hydrogen-bonded network is quite robust and determines the orientation of a variety of molecules on the surface.

Downloaded At: 16:53 21 January 2011

Acknowledgements

This work was supported by the National Science Foundation (Grants CHE-9208232, CHE-9256871 and CHE-9816380), the United States Environmental Protection Agency (Award R-822453-01-0), the Tufts University Center for Environmental Management, and the Tufts University Faculty Research Fund.

References

[1] Klassen, J., Fiehrer, K. M., and Nathanson, G. M., 1997, *J. phys. Chem.*, **101,** 9098.
[2] Saecker, M. E., and Nathanson, G., 1993, *J. chem. Phys.*, **99,** 7056.
[3] Tassotto, M., Gannon, T. J., and Watson, P. R., 1997, *J. chem. Phys.*, **107,** 8899.
[4] Baldelli, S., Schnitzer, C., Shultz, M. J., and Campbell, D., 1997, *J. phys. Chem.* B, **101,** 10435.
[5] Schnitzer, C., Baldelli, S., Campbell, D. J., and Shultz, M. J., 1999, *J. phys. Chem.* A, **103,** 6383.
[6] Baldelli, S., Schnitzer, C., Shultz, M. J., and Campbell, D. J., 1998, *Chem. Phys. Lett.*, **287,** 143.

[7] BALDELLI, S., CAMPBELL, D., SCHNITZER, C., and SHULTZ, M. J., 1999, *J. phys. Chem.* B, **103,** 2789.
[8] SCHNITZER, C., BALDELLI, S., and SHULTZ, M. J., 1999, submitted
[9] BALDELLI, S., SCHNITZER, C., and SHULTZ, M. J., 1999, *Chem. Phys. Lett.*, **302,** 157.
[10] SIMONELLI, D., BALDELLI, S., and SHULTZ, M. J., 1998, *Chem. Phys. Lett.*, **298,** 400.
[11] SCHNITZER, C., BALDELLI, S., and SHULTZ, M. J., 1999, *Chem. Phys. Lett.* (in the press).
[12] SIMONELLI, D., and SHULTZ, M. J., 1999, submitted
[13] SIMONELLI, D., and SHULTZ, M. J., 1999, submitted
[14] BALDELLI, S., SCHNITZER, C., SHULTZ, M. J., and CAMPBELL, D., 1997, *J. phys. Chem.* B, **101,** 4607.
[15] BLOEMBERGEN, N., and PERSHAN, P. S., 1962, *Phys. Rev.*, **128,** 606.
[16] SHEN, Y. R., 1989, *Ann. Rev. phys. Chem.*, **40,** 327.
[17] EISENTHAL, K. B., 1996, *Chem. Rev.*, **96,** 1343.
[18] GRAGSON, D. E., and RICHMOND, G. L., 1998, *J. phys. Chem.* B, **102,** 3847.
[19] MIRANDA, P. B., and SHEN, Y. R., 1999, *J. phys. Chem.* B, **103,** 3292.
[20] HEINZ, T. F., TOM, H. W. K., and SHEN, Y. R., 1983, *Phys. Rev.* A, **28,** 1883.
[21] HIGGINS, D. A., BYERLY, S. K., ABRAMS, M. B., and CORN, R. M., 1991, *J. phys. Chem.*, **95,** 6984.
[22] HUNT, J. H., GUYOT-SIONNEST, P., and SHEN, Y. R., 1987, *Chem. Phys. Lett.*, **133,** 189.
[23] GUYOT-SIONNEST, P., SUPERFINE, R., HUNT, J. H., and SHEN, Y. R., 1988, *Chem. Phys. Lett.*, **144,** 1.
[24] HARRIS, A. L., CHIDSEY, C. E. D., LEVINOS, N. J., and LOIACONO, D. N., 1987, *Chem. Phys. Lett.*, **141,** 350.
[25] GOH, M. C., HICKS, J. M., KEMNITZ, K., PINTO, G. R., BHATTACHARYYA, K., EISENTHAL, K. B., and HEINZ, T. F., 1988, *J. phys. Chem.*, **92,** 5074.
[26] SUPERFINE, R., HUANG, J. Y., and SHEN, Y. R., 1991, *Phys. Rev. Lett.*, **66,** 1066.
[27] DU, Q., SUPERFINE, R., FREYSZ, E., and SHEN, Y. R., 1993, *Phys. Rev. Lett.*, **70,** 2313.
[28] CASTRO, A., BHATTACHARYYA, K., and EISENTHAL, K. B., 1991, *J. chem. Phys.*, **95,** 1310.
[29] BHATTACHARYYA, K., SITZMANN, E. V., and EISENTHAL, K. B., 1988, *J. chem. Phys.*, **87,** 1442.
[30] BHATTACHARYYA, K., CASTRO, A., SITZMANN, E. V., and EISENTHAL, K. B., 1988, *J. chem. Phys.*, **89,** 3376.
[31] BELL, A. J., FREY, J. G., and VANDERNOOT, T. J., 1992, *J. chem. Soc. Faraday Trans.*, **88,** 2027.
[32] HICKS, J. M., KEMNITZ, K., EISENTHAL, K. B., and HEINZ, T. F., 1986, *J. phys. Chem.*, **90,** 560.
[33] GRUBB, S. G., KIM, M. W., RAISING, T., and SHEN, Y. R., 1988, *Langmuir*, **4,** 452.
[34] SHUANG, X., MIRANDA, P. B., KIM, D., and SHEN, Y. R., 1999, *Phys. Rev.* B, **59,** 12632.
[35] ZHANG, D., GUTOW, H., EISENTHAL, K. B., and HEINZ, T. F., 1993, *J. chem. Phys.*, **98,** 5099.
[36] DICK, B., GIERULSKI, A., MAROWSKY, G., and REIDER, G. A., 1985, *Appl. Phys.* B, **38,** 107.
[37] DICK, B., 1985, *Chem. Phys.*, **96,** 199.
[38] HIROSE, C., AKAMATSU, N., and DOMEN, K., 1992, *Appl. Spectrosc.*, **46,** 1051.
[39] HIROSE, C., AKAMATSU, N., and DOMEN, K., 1992, *J. chem. Phys.*, **96,** 997.
[40] MUENCHAUSEN, R. E., KELLER, R. A., and NOGAR, N. S., 1987, *J. opt. Soc. Am.*, **4,** 237.
[41] AKAMATSU, N., DOMEN, K., and HIROSE, C., 1992, *Appl. Spectrosc.*, **46,** 1051.
[42] MIRAGLIOTTA, J., POLIZOTTI, R. S., RABINOWITZ, P., CAMERON, S. D., and HALL, R. B., 1990, *Appl. Phys.* A, **51,** 221.
[43] MIRAGLIOTTA, J., POLIZZOTTI, R. S., RABINOWITZ, P., CAMERON, S. D., and HALL, R. B., 1990, *Chem. Phys.*, **143,** 123.
[44] HATCH, S. R., POLIZZOTTI, R. S., DOUGAL, S., and RABINOWITZ, P., 1992, *Chem. Phys. Lett.*, **196,** 97.
[45] YEGANEH, M. S., POLIZZOTTI, R. S., DOUGAL, S., and RABINOWITZ, P., 1995, *Phys. Rev. Lett.*, **74,** 1811.
[46] BALDELLI, S., SCHNITZER, C., and SHULTZ, M. J., 1998, *J. chem. Phys.*, **108,** 9817.
[47] IRISH, D. E., and BROOKER, M. H., 1981, *Advances in Infrared and Raman Spectroscopy*, edited by R. J. H. Clark and R. E. Hester (London: Heyden & Son), 212pp.

Downloaded At: 16:53 21 January 2011

[48] Bertie, J., and Lan, Z., 1996, *Appl. Spectrosc.*, **50,** 1047.
[49] Senior, W. A., and Thompson, W. K., 1965, *Nature*, **205,** 170.
[50] Schultz, J. W., and Horning, D. F., 1961, *J. phys. Chem.*, **65,** 2131.
[51] Tulk, C. A., Klug, D. D., Branderhorst, R., Sharpe, P., and Ripmeester, J. A., 1998, *J. chem. Phys.*, **109,** 8478.
[52] Scherer, J. R., Go, M. K., and Kint, S., 1974, *J. phys. Chem.*, **78,** 1304.
[53] Scherer, J. R., 1978, *Advances in Infrared and Raman Spectroscopy*, Vol. 5, edited by R. J. H. Clark and R. E. Hester (Philadelphia: Heyden), 149pp.
[54] Maréchal, Y., 1994, *J. molec. Spectrosc.*, **322,** 105.
[55] Murphy, W., 1978, *Molec. Phys.*, **36,** 727.
[56] Cummingham, K., and Lyons, P. A., 1973, *J. chem. Phys.*, **59,** 2132.
[57] Devlin, J. P., and Buch, V., 1997, *J. phys. Chem.* B, **101,** 6095.
[58] Devlin, J. P., and Buch, V., 1995, *J. phys. Chem.*, **99,** 16534.
[59] Rowland, B., Kadagathur, N. S., Devlin, J. P., Buch, V., Feldman, T., and Wojcik, M. J., 1995, *J. chem. Phys.*, **102**, 8328.
[60] Buch, V., 1999, personnal communication.
[61] Gruenloh, C. J., Carney, J. R., Hagemeister, F. C., Arrington, C. A., Zwier, T. S., Fredericks, S. Y., Wood III, J. T., and Jordan, K. D., 1998, *J. chem. Phys.*, **109,** 6601.
[62] Buck, U., 1999, personal communication.
[63] Gragson, D. E., and Richmond, G. L., 1998, *J. Am. chem. Soc.*, **120,** 366.
[64] Gragson, D. E., McCarty, B. M., and Richmond, G. L., 1997, *J. Am. chem. Soc.*, **119,** 6144.
[65] Gragson, D. E., and Richmond, G. L., 1997, *J. chem. Phys.*, **107,** 9687.
[66] Israelachvili, J., 1985, *Intermolecular Forces and Surface Forces* (San Diego: Academic Press).
[67] Chattoraj, D. K., 1981, *Ind. J. Chem.*, **20a,** 941.
[68] Adamson, A. W., and Gast, A. P., 1997, *Physical Chemistry of Surfaces* (New York: Wiley).
[69] Harkins, W. D., and McLaughlin, H. M., 1925, *J. Am. chem. Soc.*, **47,** 2083.
[70] Harkins, W. D., and Gilbert, E. C., 1926, *J. Am. chem. Soc.*, **48,** 604.
[71] Onsager, L., and Samaras, N. N. T., 1934, *J. chem. Phys.*, **2,** 528.
[72] Groenewold, J., 1997, *J. chem. Phys.*, **107,** 9668.
[73] Dietter, J., and Morgner, H., 1997, *Chem. Phys.*, **220,** 261.
[74] Benjamin, I., 1995, *Acc. chem. Res.*, **28,** 233.
[75] Randles, J. E. B., 1977, *Phys. chem. Liq.*, **7,** 107.
[76] Amirand, C., and Maillard, D., 1988, *J. molec. Struct.*, **176,** 181.
[77] Kanno, H., 1993, *J. Raman Spectrosc.*, **24,** 689.
[78] Delzeit, L., Rowland, B., and Devlin, P., 1993, *J. phys. Chem.*, **97,** 10312.
[79] Newton, M. D., and Schwartz, H. A., 1977, *J. chem. Phys.*, **67,** 5535.
[80] Librovich, N. B., Sakun, V. P., and Sokolov, N. D., 1979, *Chem. Phys.*, **39,** 351.
[81] Wilson, M., and Pohorille, A., 1991, *J. chem. Phys.*, **95,** 6005.
[82] Jarvis, N. L., and Scheiman, M. A., 1968, *J. phys. Chem.*, **72,** 74.
[83] Israelachvili, J. N., 1995, *The Handbook of Surface Imaging and Visualization*, edited by A. Hubbard (Boca Raton, Fl: CRC Press), 793pp.
[84] Burgess, J., 1978, *Metal Ions in Solution* (New York: Wiley).
[85] Du, Q., Freysz, E., and Shen, Y. R., 1994, *Phys. Rev. Lett.*, **72,** 238.
[86] Rull, F., Sobron, F., and Nielsen, O. F., 1995, *J. Raman Spectrosc.*, **26,** 663.
[87] Heyrovská, R., 1992, *Collect. Czech. Chem. Commun.*, **57,** 2209.
[88] Rull, F., 1995, *Z. Natur.* A, **50a,** 292.
[89] Heyrovská, R., 1998, personal communication.
[90] Burgess, J., 1988, *Ions in Solution* (London: Wiley).
[91] Monk, C. B., 1961, *Electrolytic Dissociation* (New York: Academic Press).
[92] Pearson, R. G., 1973, *Hard and Soft Acids and Bases* (Stroudsburg PA: Dowden, Hutchinson and Ross).
[93] Akhumov, E. I., 1974, *Zh. Pr. Khim.*, **47,** 1852.
[94] Phillips, L. F., 1994, *Aust. J. Chem.*, **47,** 91.
[95] Fairbrother, D. H., Johnston, H., and Somerjai, G., 1996, *J. phys. Chem.*, **100,** 13696.
[96] Radüge, C., Pflumio, V., and Shen, Y. R., 1997, *Chem. Phys. Lett.*, **274,** 140.

Downloaded At: 16:53 21 January 2011

[97] ZHANG, R., WOOLDRIDGE, P. J., ABBATT, J. P. D., and MOLINA, M. J., 1993, *J. phys. Chem.*, **97,** 7351.
[98] MARTIN, S. T., SALCEDO, D., MOLINA, L., and MOLINA, M. J., 1997, *J. phys. Chem.* B, **101,** 5307.
[99] MINER, C. S., and DALTON, N. N., 1953, *Glycerol* (New York: Reinhold Publishing Corp).
[100] CHATTORAJ, D. K., and MOULIK, S. P., 1977, *Ind. J. Chem.*, **15a,** 73.
[101] SEXTON, B. A., and MITCHELL, G. E., 1980, *Surf. Sci.*, **99,** 532.
[102] BENNDORF, C., and MADEY, T. E., 1983, *Surf. Sci.*, **135,** 164.
[103] CEYER, C. T., and YATES, J. T. JR, 1985, *Surf. Sci.*, **155,** 584.
[104] CHATTOPADHYAY, A., YANG, H., and WHITTEN, J. L., 1990, *J. phys. Chem.*, **94,** 6379.
[105] PANELLA, V., SUZANNE, J., and COULOMB, J.-P., 1996, *Surf. Sci.*, **350,** L211.
[106] AMORES, J., ESCRIBANO, V., RAMIS, G., and BUSCA, G., 1997, *Appl. Catal.* B, **13,** 45.
[107] WU, M.-C., TRUONG, C. M., and GOODMAN, D. W., 1993, *J. phys. Chem.*, **97,** 4182.
[108] MOCUTA, D., AHNER, J., and YATES, J. T. JR, 1997, *Surf. Sci.*, **383,** 299.
[109] QUINN, P. K., ASHER, W. E., and CHARLSON, R. J., 1992, *J. atmos. Chem.*, **14,** 11.
[110] DENTENER, F. J., and CRUTZAN, P. J., 1994, *J. atmos. Chem.*, **19,** 331.
[111] FINLAYSON-PITTS, B. J., and PITTS, J. N. JR, 1986, *Atmospheric Chemistry, Fundamental and Experimental Techniques* (New York: Wiley).
[112] RICE, O. K., 1928, *J. phys. Chem.*, **32,** 583.
[113] HERZBERG, G., 1945, *Molecular Spectra and Molecular Structure II. Infrared and Raman Spectra of Polyatomic Molecules* (New York: Van Nostrand Reinhold).
[114] FISCHER, W. B., and EYSEL, H.-H., 1997, *J. molec. Struct.*, **415,** 249.
[115] POUTHIER, V., RAMSEYER, C., and GIRARDET, C., 1998, *J. chem. Phys.*, **108,** 6502.

Downloaded At: 16:53 21 January 2011